ORBITAL VELOCITIES IN IRREGULAR WAVES

by

F.C. VIS

Project Engineer

Delft Hydraulics Laboratory

The Netherlands

1 ABSTRACT

Experimental and theoretical study to determine the applicability of li-
near wave theory for the description of the velocity field in irregular
waves. A comparison between theory and measurement was executed both in
frequency and in time domain. In frequency domain by means of the experi-
mentally and theoretically determined frequency response functions of
wave motion to orbital velocity, and in time domain by means of the mea-
sured and computed time records of the velocities. The time records for
the velocities were computed from the measured waterlevel fluctuations
by using the impuls response function method. The orbital velocities
were measured contactless with laser-doppler equipment.

2 INTRODUCTION

In order to determine the applicability of linear wave theory for conver-
sion of irregular wave motion to wave induced orbital velocities near
the bottom, the Delft Hydraulics Laboratory has carried out in the past
experimental investigation where the velocities were measured by means of
a propeller-type flowmeter. The results of this study were used for the
computation of wave forces on submarine pipelines. Although'in general a-
a reasonable agreement was found between theory and measurement, also
significant discrepancies were observed. However, these discrepancies
had to be ascribed to the distortion of the flow by the flowmeter.

The development of the laser-doppler velocity meter made it possible to
measure accurately the orbital velocities in an extremely small area,
without influence of the meter. With this accurate instrument new expe-
riments in irregular waves were carried out, where apart from the bottom
velocity also the horizontal and vertical orbital velocities at half wa-
ter depth and just beneath the deepest trough were measured. The program

comprised waves of moderate steepness at intermediate depth/wavelength ratios ($0.008 < h/g\,T_p^2 < 0.069$, $0.0009 < H_s/g\,T_p^2 < 0.0064$). It appeared that the discrepancies mentioned above were indeed due to inaccuracies of the flowmeter and that the agreement with linear wave theory was even better than was found in the first set of experiments.

3 NOTATION

a	distance from the bottom where the velocities were measured
a_{cs}	significant crest of the waves
a_{c1}	crest exceeded by 1% of all the crests of the wave record
a_{ts}	significant trough of the waves
a_{t1}	trough exceeded by 1% of all the troughs of the wave record
g	acceleration of gravity
h	water depth
$H(\omega)$	computed frequency response function
$\hat{H}(\omega)$	"measured" frequency response function
$h(\tau)$	impuls response function
H_s	significant wave height
H_1	wave height exceeded by 1% of all the heights of the wave record
i	$\sqrt{-1}$
k	wave number
$S_{xy}(\omega)$	cross-spectrum
$S_{xx}(\omega)$	auto-spectrum
u_{cs}	significant crest velocity of the horizontal velocity component u
u_{c1}	crest velocity exceeded by 1% of all the crest velocities of the record of the horizontal velocity component u
u_{ts}	significant trough velocity of the horizontal velocity component u
u_{t1}	trough velocity exceeded by 1% of all the trough velocities of the record of the horizontal velocity component u
v_{cs}	significant crest velocity of the vertical velocity component v
v_{c1}	crest velocity exceeded by 1% of all the crest velocities of the record of the vertical velocity component v
v_{ts}	significant trough velocity of the vertical velocity component v
v_{t1}	trough velocity exceeded by 1% of all the trough velocities of the record of the vertical velocity component v
ε	relative error

4 THEORETICAL APPROACH

In Appendix A it is shown that according to the linear wave theory the water level fluctuations $\eta(t)$ and the horizontal and vertical orbital velocity components $u(t)$ and $v(t)$ at distance a from the bottom are mutually related by

$$u(t) = \int_0^\infty h_u(\tau) \{\eta(t-\tau) + \eta(t+\tau)\} \, d\tau \tag{1}$$

$$v(t) = \int_0^\infty h_v(\tau) \{\eta(t-\tau) - \eta(t+\tau)\} \, d\tau, \tag{2}$$

where $h_u(\tau)$ and $h_v(\tau)$ are impulse response functions.
The corresponding frequency response functions are given by

$$H_u(\omega) = \frac{\omega \cosh ka}{\sinh kh} \tag{3}$$

$$H_v(\omega) = i \frac{\omega \sinh ka}{\sinh kh}. \tag{4}$$

The "measured" frequency response functions $\hat{H}_u(\omega)$ and $\hat{H}_v(\omega)$ can be
obtained from the measured data by using the relation

$$\hat{H}(\omega) = \frac{S_{xy}(\omega)}{S_{xx}(\omega)}, \tag{5}$$

where $S_{xy}(\omega)$ is the cross-spectrum of input (wave motion) and output
(orbital velocity component) and $S_{xx}(\omega)$ is the auto-spectrum of input
(see e.g. Bendat and Piersol, 1971).

5 MEASUREMENTS

5.1 Experimental Set-up

The tests were carried out in the 2 meter wide windwave flume of the
Delft Hydraulics Laboratory. In this flume irregular waves can be gen-
erated up to a height of 30 cm by means of wind and/or a hydraulically
driven wave generator. A detailed description of the wave generator is
given in (DHL, 1976). For the actual tests no wind was applied. The
water level fluctuations were measured by means of a resistance type
wave height meter, consisting of two vertical metal rods, and the
orbital velocities were measured by means of a laser-doppler equipment
which could simultaneously measure horizontal and vertical component.
A description of the laser-doppler velocity meter is given in (Godefroy,
1978). In order to measure the undisturbed velocities with this instru-
ment, the walls of the flume had to be translucent for transmitting the
laser beams. As this was not the case, the flume was partially provided
with an inner flume with perspex walls (see Figure 1). For absorption
of the waves, beaches were used with a slope of 1:10 for minimal re-
flection.
Wave motion and orbital velocities were simultaneously measured in the
same cross-section of the flume at a mutual distance of 20 cm. This
distance proved to be sufficient for avoiding disturbance of the veloc-
ity measurement by the wave height meter. As the waves were long-
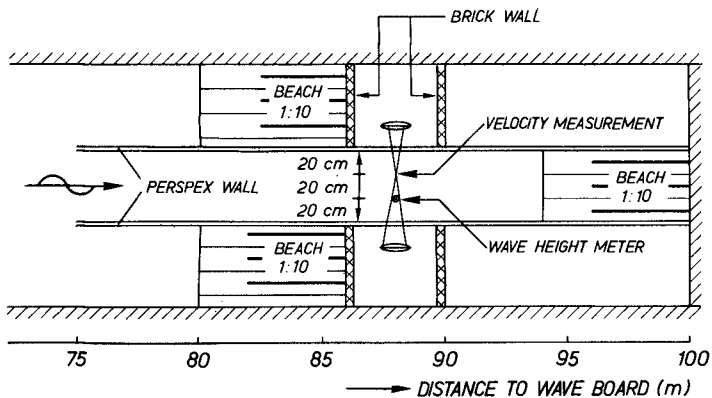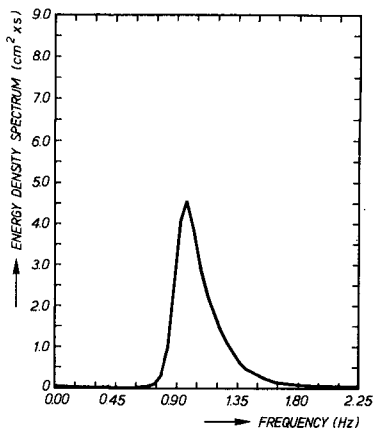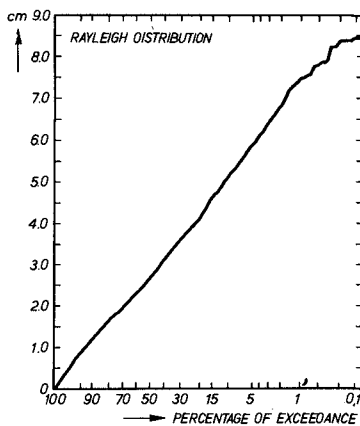crested this solution could be used.

Fig. 1 Lay-out of the 2 m wide wind wave flume

$M_{0\eta}$ $= 143\ cm^2$

$4\sqrt{M_{0\eta}}$ $= 4.78\ cm$

T_p $= 1.02\ s$

Fig. 2 Wave spectrum at test 16

H_s $= 4.73\ cm$

$H_{z.max} = 8.83\ cm$

Fig. 3 Wave height distribution at test 16

For elaboration with the computer the measured signals were digitized
with sample frequency of 25 Hz.

5.2   Test Program

The test program comprised irregular waves of moderate steepness at
intermediate depth/wave length ratios, which are the normal working
conditions for offshore structures. The wave parameters are given in
Tables I and II. The wave heights, defined as the maximum difference of
the record between two succeeding zero-down crossings, appeared to be
nearly Rayleigh distributed. As an example the energy density spectrum
of a wave record and the corresponding cumulative frequency distribu-
tion of the wave heights at test 16 are presented in Figures 2 and 3.
Velocities were measured at three locations along the vertical: the
horizontal bottom velocity just outside the boundary layer, and the
horizontal and vertical components at mid-depth and just beneath the
deepest trough (see Tables I and II).

TABLE I   TEST PROGRAM FOR   TABLE II   TEST PROGRAM FOR VELOCITIES
          BOTTOM VELOCITIES   AT DISTANCE a FROM THE BOTTOM

TEST	$\dfrac{1000\ h}{g\ T_p^2}$	$\dfrac{1000\ H_s}{g\ T_p^2}$	ε_u %
1	7.8	0.89	1.4
2	11.8	0.88	5.2
3	19.2	1.75	2.1
4	19.2	2.49	2.3
5	24.4	2.02	1.7
6	24.4	2.81	2.2
7	26.3	3.13	4.8
8	26.3	3.12	2.8
9	33.5	2.69	1.2
10	33.5	3.94	2.6
11	43.6	3.85	5.8
12	43.6	5.62	2.9

TEST	$\dfrac{1000\ h}{g\ T_p^2}$	$\dfrac{1000\ H_s}{g\ T_p^2}$	$\dfrac{a}{h}$	ε_u %	ε_v %
13	13.3	1.3	0.500	2.0	4.4
14	13.3	1.3	0.873	2.9	2.1
15	16.3	2.0	0.500	4.7	7.6
16	16.3	2.0	0.825	1.4	3.5
17	17.0	1.5	0.500	3.5	3.1
18	20.6	1.6	0.850	3.0	2.6
19	39.2	4.8	0.500	3.2	7.1
20	39.2	4.6	0.825	1.4	3.4
21	53.9	5.2	0.500	5.2	5.4
22	53.9	5.0	0.873	0.6	2.1
23	68.6	5.2	0.500	4.6	2.8
24	68.6	5.3	0.850	1.0	1.7
25	35.9	6.4	0.810	1.0	1.2

6   COMPARISON OF THEORY AND MEASUREMENT

The comparison of the measured velocities in irregular waves with the
linear wave theory has been carried out in frequency domain and, except
for the bottom velocities, also in time domain.
In frequency domain theory and measurement were compared by defining a
relative error ε by

$$\varepsilon = \frac{1}{N} \sum_{i=1}^{N} \left| \frac{\left| \hat{H}(\omega_i) \right| - \left| H(\omega_i) \right|}{\left| H(\omega_i) \right|} \right| ,$$

where the "measured" frequency response functions $\hat{H}(\omega_i)$ were determined
by (5), and $H(\omega_i)$ by means of (3) or (4). The notation $|.|$ denotes the

amplitude of the (complex) number. The relative errors ε have been
evaluated only for those frequencies ω_i for which both the spectral
density functions of input and output were greater than 10% of their
peak value, as for smaller values the spectral densities are relatively
inaccurate. All spectra were computed using a Fast Fourier Transform
method. The relative errors are given in Tables I and II. The indices u
and v have been attached for distinction between horizontal and verti-
cal velocity.
Figure 4 presents most amplitudes of the "measured" and computed
frequency response functions.

A comparison in time domain was executed for the velocities above the
bottom by computing the time records of the orbital velocity components,
for which either (1) or (2) was used, and by comparing them with the
measured ones. The significant and the 1% crest and trough velocities
are presented in Tables III and IV. Crest and trough velocities are
defined in accordance with crests and troughs of the wave motion by the
maximum positive and maximum negative velocity between two succeeding
zero-down crossings. A positive velocity means for the horizontal veloc-
ity a velocity in direction of propagation of the waves, and for the
vertical velocity a velocity in upwards direction.
An example of measured and computed time record is presented in Figure
5 and in more detail in Figure 6.

TABLE III   WAVE MOTION AND MEASURED AND COMPUTED HORIZONTAL ORBITAL
            VELOCITY

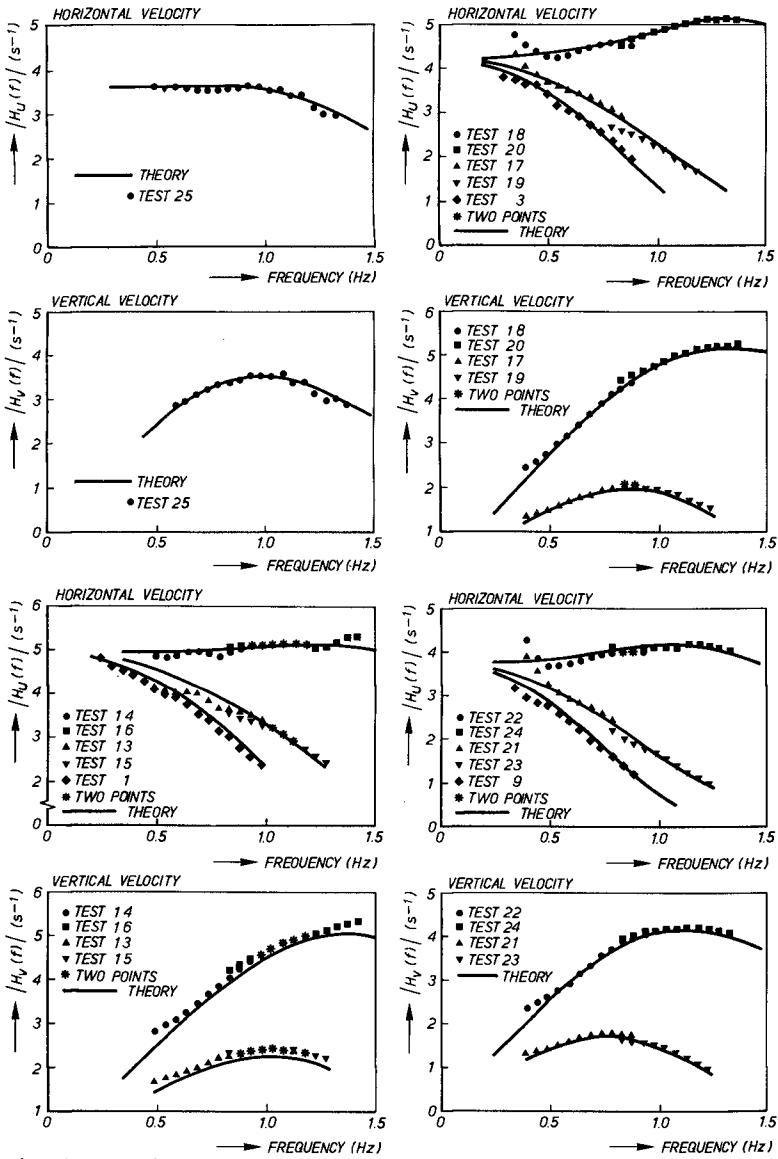| TEST | WAVE MOTION MEASURED | | | | HORIZONTAL ORBITAL VELOCITY | | | | | | | |
| | | | | | MEASURED | | | | COMPUTED | | | |
	a_{cs} cm	a_{cl} cm	a_{ts} cm	a_{tl} cm	u_{cs} cm/s	u_{cl} cm/s	u_{ts} cm/s	u_{tl} cm/s	u_{cs} cm/s	u_{cl} cm/s	u_{ts} cm/s	u_{tl} cm/s
13	2.5	3.9	2.4	3.5	9.0	12.6	9.4	14.2	9.0	12.7	9.9	14.9
14	2.4	3.6	2.7	3.5	11.7	16.5	12.0	18.3	11.6	16.8	12.2	18.4
15	2.6	3.9	2.4	3.6	7.6	11.5	7.7	13.1	6.8	10.6	8.1	13.0
16	2.5	4.0	2.3	3.6	12.0	17.8	12.4	20.8	12.0	18.6	12.2	18.6
17	2.8	4.0	2.6	4.0	9.6	13.2	9.5	16.0	9.5	13.3	9.6	16.1
18	2.8	3.8	2.7	4.1	12.6	17.0	11.5	17.2	12.6	17.0	12.0	17.2
19	2.9	4.8	2.5	4.0	5.9	9.1	5.9	10.0	5.6	9.4	5.9	9.3
20	2.7	4.5	2.5	3.8	12.0	19.1	12.9	20.4	12.7	21.0	12.3	18.8
21	3.5	5.2	3.2	4.6	10.1	14.6	10.1	16.2	9.6	14.9	9.8	14.5
22	3.0	4.5	2.8	4.0	10.8	16.1	11.5	16.9	11.8	17.4	11.0	16.0
23	2.7	4.6	2.7	4.1	4.2	6.1	4.1	6.8	4.1	6.5	4.3	6.7
24	2.9	4.5	2.6	3.8	10.6	15.3	11.8	18.4	11.2	17.0	11.1	16.4
25	7.3	13.1	6.2	9.6	22.0	34.0	25.1	41.2	23.1	36.2	24.6	40.5

Fig. 4 Comparison of measured and computed frequency response function
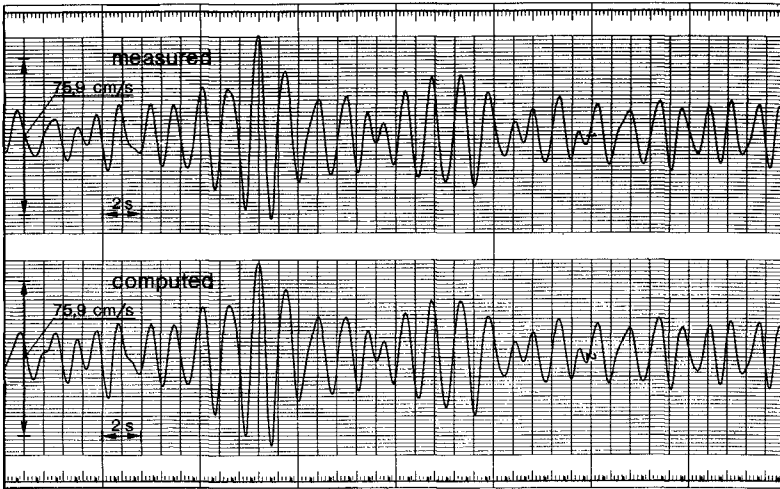
Fig. 5 Time records of measured and computed horizontal orbital velocity
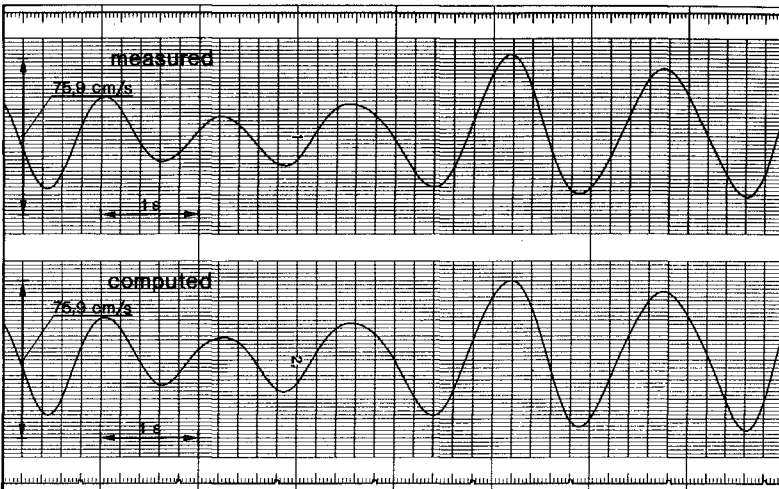   component at test 25

Fig. 6 Time records of measured and computed horizontal orbital velocity
        component at test 25 in more detail

TABLE IV MEASURED AND COMPUTED VERTICAL ORBITAL VELOCITY

| TEST | VERTICAL ORBITAL VELOCITY | | | | | | | |
| | MEASURED | | | | COMPUTED | | | |
	v_{cs} cm/s	v_{cl} cm/s	v_{ts} cm/s	v_{tl} cm/s	v_{cs} cm/s	v_{cl} cm/s	v_{ts} cm/s	v_{tl} cm/s
13	5.2	7.8	5.2	7.5	4.9	7.0	4.8	7.0
14	9.2	14.2	9.0	13.3	9.0	13.2	8.7	12.9
15	5.7	9.0	5.8	8.9	5.3	8.3	5.3	8.1
16	11.2	18.3	11.4	17.8	11.0	17.7	11.1	17.9
17	4.4	6.3	4.6	6.6	4.2	6.1	4.3	6.4
18	8.7	12.9	8.4	12.6	8.6	12.6	8.8	12.4
19	4.7	8.0	4.9	7.9	4.6	7.5	4.6	7.3
20	12.2	19.9	12.3	19.4	12.1	19.9	12.1	19.2
21	4.9	7.6	5.6	7.8	5.0	7.6	5.0	7.3
22	9.1	14.5	9.0	13.9	9.0	14.3	8.9	13.4
23	3.7	5.7	3.7	5.8	3.6	5.7	3.6	5.8
24	11.0	16.4	11.0	17.0	10.8	16.5	10.8	16.8
25	21.0	34.7	20.9	32.8	20.8	35.6	21.2	33.0

7 DISCUSSION OF THE RESULTS

It is remarkable to see from the comparison in frequency domain that
the velocities near the free surface match linear wave theory better
than the velocities at mid-depth, whereas in view of testresults in
regular waves (see e.g. Le Méhauté, Divoky and Lin, 1968) just the
opposite would be expected. This phenomenon was observed for both the
orbital velocity components. The bottom velocities were indeed in more
agreement with linear wave theory than the velocities at mid-depth.
However, from the comparison in time domain, as far as executed, these
tendencies could not be observed.

From Table III it appears that for the horizontal velocities the trough
velocities are greater in magnitude than the crest velocities, contrary
to the wave motion where the crests are higher than the troughs. The
vertical velocities appeared to be distributed more symmetrically. It
is important to note that these tendencies are followed by linear wave
theory in most cases. However, when a higher order wave theory, such as
the fifth order Stokes' method of De (1954), would be used for descrip-
tion of the velocity field in the individual waves of the irregular sea
(the so-called deterministic approach) just the opposite would be found,
apart from the fact that with respect to the crests of the waves only a
"symmetrical" velocity distribution would be found. Also when linear
wave theory is used in the random phase model, these tendencies will
not be found, just as a consequence of the random phases by which equal
crest and trough velocities will be found.

8 CONCLUSIONS AND RECOMMENDATIONS

In the present study low to moderately steep irregular waves have been

investigated, and it appeared that linear wave theory gives a reasonable
description of the velocity field, in particular for the velocities near
the free surface just beneath the deepest trough.
In view of these results it is advised to carry out further investiga-
tion of the applicability of linear wave theory to more severe wave
conditions and to the velocities in the crests of the waves.
It will also be interesting to check linear wave theory for a spatial
description of the velocity field. As for long-crested waves the corre-
lation between water level fluctuations and orbital velocities in the
same vertical has now been shown, this investigation can then be re-
stricted to a check of the correlation in space of the wave motion at
different locations. This was already investigated by Lundgren and Sand
(1978), who found that the dispersion of the waves over limited distance
is well described by linear wave theory, but that deviations increase
with increasing distance. For directional seas research of the velocity
field is necessary.

9 REFERENCES

BENDAT, J.S. and PIERSOL, A.G. (1971).
Random data: Analysis and measurement procedures.
New York, Wiley.

DE, S.C. (1955).
Contributions to the study of Stokes waves.
Proc. Camb. Phil. Soc.

DELFT HYDRAULICS LABORATORY (1976).
Random wave generation of research on immersed marine vehicles.
Publication no. 167.

GODEFROY, H.W.H.E. (1978).
Application of the Laser-Doppler velocity measurement in open and closed
conduits.
Proc. of Flomeko 1978, Groningen, The Netherlands.

LE MEHAUTE, B., DIVOKY, D. and LIN, A. (1968).
Shallow water waves. A comparison of theory and experiment.
Proc. Eleventh International Conference on Coastal Engineering.

LUNDGREN, H. and SAND, S.E. (1978).
Natural wave trains: Description and reproduction.
Proc. Sixteenth International Conference on Coastal Engineering.

APPENDIX A. THEORY OF LINEAR SYSTEMS

Suppose that $x(t)$ is the input and $y(t)$ the output or response of a
linear system and that $X(\omega)$ and $Y(\omega)$ are the corresponding Fouriertrans-
forms. Put $H(\omega)$ equal to the ratio $Y(\omega)/X(\omega)$; thus

$$Y(\omega) = H(\omega).X(\omega) \qquad\qquad (A.1)$$

Inverse Fouriertransform of this relation yields the well-known convolution expression

$$y(t) = \int_{-\infty}^{+\infty} h(\tau)\ x(t-\tau)\ d\tau\ , \qquad\qquad\qquad (A.2)$$

where h(t) is the inverse Fouriertransform of $H(\omega)$, given by

$$h(t) = \frac{1}{2\pi} \int_{-\infty}^{+\infty} H(\omega)\ e^{i\omega t}\ d\omega \qquad\qquad\qquad (A.3)$$

Often h(t) is denoted by impuls response function, as

$$h(t) = \int_{-\infty}^{+\infty} h(\tau)\ \delta(t-\tau)\ d\tau\ ,$$

and $H(\omega)$ by frequency response function.

Expression (A.1) yields the relation between input and output of the linear system in frequency domain and (A.2) in time domain. Thus if the frequency response function $H(\omega)$ of the linear system is known, then the response y(t) on any arbitrary input can be computed, either by using (A.3) followed by (A.2), or by using (A.1), in which case first the input has to be Fouriertransformed, resulting in $X(\omega)$, and the output $Y(\omega)$ has to be Fourier inverted in order to obtain y(t).

The frequency response function between wave motion and orbital velocity component at distance a from the bottom (both in the same cross-section of the flume) can be found with linear wave theory by putting as input of the linear system the wave motion in frequency domain

$$X(\omega) = e^{i\omega t} = \cos\omega t + i\ \sin\omega t\ . \qquad\qquad (A.4)$$

(Note that $e^{i\omega t}$ is the Fouriertransform of the impulse on time $-t$; t has to be considered as a parameter.)
According to linear wave theory the response $Y(\omega)$ is then given by

$$Y(\omega) = \frac{\omega\ \cosh\ ka}{\sinh\ kh}\ e^{i\omega t} \qquad\qquad\qquad (A.5)$$

for the horizontal orbital velocity component, which is defined positive in wave direction, and by

$$Y(\omega) = i\ \frac{\omega\ \sinh\ ka}{\sinh\ kh}\ e^{i\omega t} \qquad\qquad\qquad (A.6)$$

for the vertical orbital velocity component, which is defined positive in upwards direction.
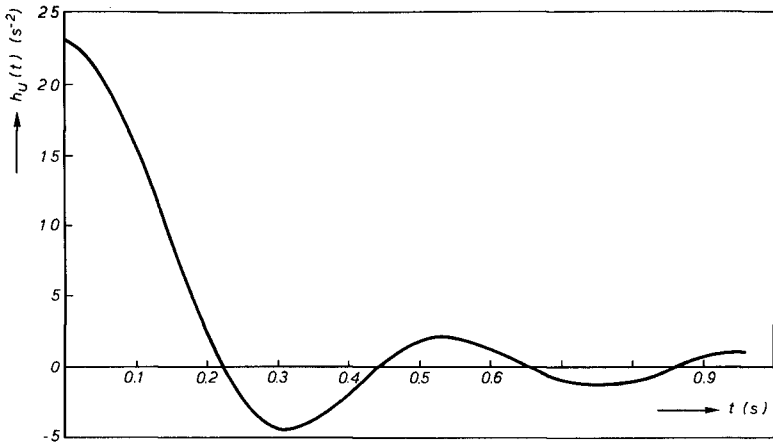Then by using (A.1) the frequency response functions can be determined to be

Fig. 7 Impuls response function for the horizontal orbital
       velocity component at test 14 and 16.
       ω_o = 15 rad/s, t_o = 4.0 s

$$H_u(\omega) = \frac{\omega \cosh ka}{\sinh kh} \tag{A.7}$$

$$H_v(\omega) = i \frac{\omega \sinh ka}{\sinh kh} \; , \tag{A.8}$$

where indices u and v have been attached for distinction.
With the aid of (A.3) it follows that

$$h_u(t) = \frac{1}{\pi} \int_0^\infty \left\{ \frac{\omega \cosh ka}{\sinh kh} \cos\omega t \right\} d\omega \; , \tag{A.9}$$

$$h_v(t) = \frac{1}{\pi} \int_0^\infty \left\{ \frac{\omega \sinh ka}{\sinh kh} \sin\omega t \right\} d\omega \; , \tag{A.10}$$

where also use was made of the property that the impuls response of a
physical system is real.
From these expressions it can be seen that $h_u(t)$ is an even and $h_v(t)$ an
odd function of t. With these properties it follows from (A.2) that the
horizontal and vertical orbital velocity components u and v at distance
a from the bottom are respectively given by

$$u(t) = \int_0^\infty h_u(\tau) \left\{ \eta(t-\tau) + \eta(t+\tau) \right\} d\tau \tag{A.11}$$

$$v(t) = \int_0^\infty h_v(\tau) \left\{ \eta(t-\tau) - \eta(t+\tau) \right\} d\tau \tag{A.12}$$

It is remarkable to see from these relations that the response on time
t depends on the wave motion $\eta(t)$ before and after t. Thus, not only
the past but also the future of $\eta(t)$ determines the velocities at time t.
Physically seen this is rather strange. However, it has to be realized
that these relations are based on linear wave theory where it is assumed
that the sinusoidal wave motion is present from $t = -\infty$ to $t = +\infty$. In
view of this basic assumption, the results (A.11) and (A.12) could be
expected.

In order to achieve existing integrals in (A.9) and (A.10), the con-
stituent functions $H_u(\omega)$ and $H_v(\omega)$ have been put equal to zero for
$\omega > \omega_0$, which implies that the response on input in this frequency
range is zero. However, this interference is no limitation if ω_0 is
chosen such that for higher frequencies the input signal does not con-
tain energy.
For numerical computation of the integrals in (A.11) and (A.12), the
functions $h_u(t)$ and $h_v(t)$, which approach to zero for $t \to \infty$, have been
put equal to zero for $t > t_0$, where t_0 is chosen such that for $t > t_0$

$$|h(t)| < \varepsilon . \max_p |h(p)|$$

(e.g.   is 0.01). An example of $h_u(t)$ is presented in Figure 7.